Strongly Coupled Stimulated Raman Backscatter from Subpicosecond Laser-Plasma Interactions

C. B. Darrow, C. Coverdale, and M. D. Perry
Lawrence Livermore National Laboratory, Box 808, Livermore, California 94550

W. B. Mori, C. Clayton, K. Marsh, and C. Joshi
Department of Electrical Engineering, University of California, Los Angeles, California 90024
(Received 24 April 1992)

We have observed strongly coupled stimulated Raman backscatter from the interaction of an intense, subpicosecond laser with an underdense plasma. The strongly coupled backscatter spectra have widths greater than the plasma frequency, extend to the blue side of the laser frequency, and, at the highest densities, are shifted by less than ω_p. These observations are consistent with the predictions of a strongly coupled Raman theory, appropriately modified for short laser pulses.

PACS numbers: 52.35.Mw, 52.40.Nk, 52.50.Jm

Stimulated Raman backscattering (RBS) in plasmas is a wave-wave interaction process in which an incident electromagnetic wave (ω_0,k_0) decays into a longitudinal electrostatic plasma wave (ω_{es},k_{es}) and a backscattered electromagnetic wave (ω_1,k_1). RBS has long been a topic of interest in laser-driven inertial confinement fusion [1,2] and, more recently, in subpicosecond laser-plasma interactions. For example, RBS may reduce the efficiency of proposed recombination x-ray lasers [3] and, for relativistic quiver velocities, the odd harmonics produced by RBS may provide a tunable short-wavelength source [4].

In this Letter we report experimental observations of RBS produced by a subpicosecond laser. RBS from ultrashort-pulse lasers interacting with plasmas differs from that observed in long-pulse experiments. First, the laser pulse duration can be comparable to the instability growth time. Second, the pulse length is typically a fraction of the Rayleigh length and hence the plasma length in experiments where the laser creates the plasma by ionizing an ambient gas. In such cases the intensity of the backscattered light depends on the number of e-foldings undergone as it travels back through the laser pulse, while the scattered pulse length, and thus the total scattered energy, depends on the length of the plasma, not the pulse duration. Third, the peak quiver velocity defined nonrelativistically of an electron in the laser field, $v_{osc}=eE_{laser}/m\omega_{laser}$, can approach or exceed the speed of light, leading to instability growth rates greater than ω_p. Here $\omega_p=(4\pi n_e^2/m_e)^{1/2}$ is the electron plasma frequency. In this regime neither the longitudinal nor the electromagnetic decay waves are normal modes. We will show that this results in a backscatter spectrum exhibiting a very broad spectral feature redshifted with respect to the incident laser by roughly ω_p with a component that extends to the blue side of the laser. Finally, the laser pulse is sufficiently short to justify the neglect of ion motion.

In conventional RBS the electromagnetic pump, the backscattered electromagnetic wave, and the electrostatic wave obey the frequency and wave-number matching conditions $\omega_{es}=\omega_0-\omega_1$ and $\mathbf{k}_{es}=\mathbf{k}_0-\mathbf{k}_1$. At low intensities [5], $v_{osc}/c<2\sqrt{2}(\omega_p/\omega_0)^{1/2}$, the instability has its largest growth rate when $(\omega_1,\mathbf{k}_1)$ and $(\omega_{es},\mathbf{k}_{es})$ satisfy their respective dispersion relations. Consequently, for $k_{es}^2\lambda_D^2<1$ and $\omega_p\ll\omega_0$, the peak of the backscattered spectrum is redshifted by the Bohm-Gross frequency

$$\omega_{BG}=\omega_p\left(1+\frac{12\omega_0^2}{\omega_p^2}\frac{kT_e}{mc^2}\right)^{1/2},$$

where T_e is the electron temperature and λ_D is the Debye length. Furthermore, the frequency range of the unstable modes is equal to twice the maximum temporal growth rate, $\gamma_0=\frac{1}{2}(v_{osc}/c)(\omega_0\omega_p)^{1/2}$, which is less than ω_p. For arbitrarily (but nonrelativistic) large intensities, the warm fluid dispersion relation can be solved numerically for the complex frequency ω_{es} of the fastest growing mode. In Fig. 1(a) the imaginary part of ω_{es}, ω_i, is plotted against the real part of ω_{es}, ω_r, for a low-intensity $(v_{osc}/c=0.1)$ and a high-intensity $(v_{osc}/c=0.8)$ case. The range of unstable frequencies is seen to be markedly different when the instability is driven in the high-

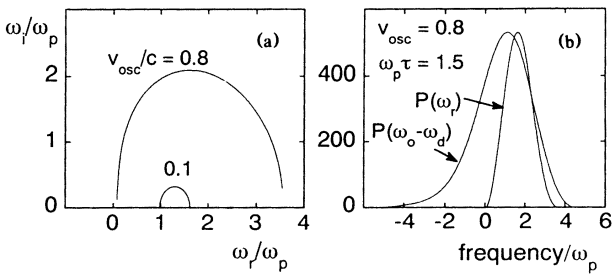

FIG. 1. (a) Numerical solutions to the cold-plasma SRS dispersion relation for two pump strengths, v_{osc}/c, approximating those used in the experiments. ω_i (ω_r) is the imaginary (real) part of the complex electrostatic mode frequency. (b) Theoretically predicted strongly coupled RBS spectra for a growth time of $\omega_0 t=81$, growth rates from (a), and a density of $\omega_0/\omega_p=54.6$. (ω_r and ω_d are explained in the text.)

intensity regime. As the intensity is increased, the maximum temporal growth rate, $\gamma_0 = \max(\omega_i)$, approaches and eventually exceeds ω_p while ω_r becomes increasingly larger than ω_{BG}. When γ_0 substantially exceeds ω_p, $\gamma_0 = \sqrt{3}\omega_r = \sqrt{3}(\omega_p^2 \omega_0 v_0^2/16c^2)^{1/3}$ and the instability is said to be strongly coupled [5]. The width of the ω_i vs ω_r curve is approximately twice the maximum temporal growth rate as can also be seen in Fig. 1(a).

In strongly coupled RBS the waves must still obey ω and k matching in order for the instability to grow exponentially. However, the frequency and wave number of the plasma wave, and therefore those of the light wave, do not satisfy their respective dispersion relations. When an extremely short laser pulse excites these strongly driven modes they exponentiate from the leading edge backward through the laser pulse. The growth rate in the short-pulse variable $z-ct$ is given by $\omega_i = \omega_r = (\omega_p^2 \omega_0 v_0^2/10c^2)^{1/3}$ which is only 0.67 times smaller than the temporal growth rate [6]. When the backscattered wave exits the laser pulse before it exits the plasma (since plasma length is much greater than the laser pulse length) it must couple to a normal mode in the pump-free plasma. In this situation the exit boundary (i.e., the envelope of the laser) is moving and causes both the frequency and the wave number of the backscattered wave to change when it leaves the laser pulse. Thus the experimentally detected frequency ω_d will in general be different from ω_1 and the usual strong-coupling theory must be modified.

The detected frequency for each unstable ω_1 and k_1 can be determined by requiring that the electric and magnetic fields be continuous at some point near the trailing edge of the laser pulse where the instability stops growing. The fields can be continuous only if the continuity of the phase condition

$$\omega_d t + k_d z = \omega_1 t + k_1 z + c_1 \tag{1}$$

is satisfied for all times at the moving boundary. The position of the moving boundary is given by $z = z_0 + v_g t$, where v_g is the group velocity of the envelope and $c_1 = (k_d - k_1) z_0$. After substituting the boundary position for z, Eq. (1) becomes

$$\omega_d + k_d v_g = \omega_1 + k_1 v_g . \tag{2}$$

Since ω_d and k_d satisfy the electromagnetic dispersion relation in a plasma, we use $ck_d = (\omega_d^2 - \omega_p^2)^{1/2}$ and Eq. (2) becomes a quadratic equation for ω_d. Defining $\delta = (k_0 - k_1)c$ and ω_r for the real part of ω_{es} we obtain, for $\omega_p \ll \omega_0$, the detected frequency of the backscattered wave

$$\omega_d \cong \omega_0 - \tfrac{1}{2}(\delta + \omega_r) . \tag{3}$$

It can be seen from Eq. (3) that, for low intensity, the detected frequency reduces to the standard result $\omega_d = \omega_0 - \omega_{BG}$. However, in the strongly coupled limit δ approaches zero for the most unstable modes and can become negative in some cases. Therefore, at high densities the redshift for the mode with the maximum growth rate, $\sim\omega_r/2$, can be less than ω_p, and for all densities ω_d can be larger than ω_0 even though ω_r is positive. We stress that this last point does not violate action (photon) conservation because the generation of the observed spectra is a two-step process. First ω_1 and k_1 are created by the RBS instability which does conserve action. Second, this mode is frequency upshifted as it is transmitted through the laser pulse. This process is analogous to the frequency upshifting encountered in the interaction of light with underdense ionization fronts in that action need not be conserved [7].

In order to obtain theoretical spectra we numerically solve the warm fluid RBS dispersion to find δ for each ω_i and ω_r shown in Fig. 1(a). We then calculate the growth rate in terms of ω_d. A white-noise source is then exponentiated for both the ω_i vs ω_d and the ω_i vs $\omega_0 - \omega_r$ curves. This is shown in Fig. 1(b) where the exponentiation time is $\omega_0 t = 81$ and the spectral power is plotted as a function of both ω_r [$P(\omega_r)$] and ω_d [$P(\omega_d)$]. The relative shape of these curves is not sensitive to the choice for the exponentiation time. These curves reveal two surprising results. First, the detected spectrum $P(\omega_d)$ is significantly wider than the peak growth rate and second, although no modes growing inside the laser pulse are blueshifted, a portion of the *detected* spectrum can be blueshifted with respect to the laser frequency.

In the experiments Nd:glass laser pulses, 0.8 psec (FWHM) in duration containing up to 4 J of 1.05 μm light [8], were focused by an $f/8$ lens for a maximum peak focal intensity of 10^{18} W/cm^2 ($v_{osc} = 0.8$) [9]. The prepulse intensity contrast was about 10^{-3} with a duration of about 300 ps. In the experiments reported here, although the ionization dynamics and heating may be affected, the RBS interaction at high intensities is not believed to be significantly influenced by the prepulse.

Because the tunneling ionization rate is high even very early in the laser pulse (Keldysh parameter $\kappa \cong 0.2$ at $10^{-2} I_{peak}$), calculations using the Keldysh ionization rate, as well as plasma images [10], suggest that plasma is formed as far as 15 Rayleigh lengths ($z_0 \sim 500$ μm) on either side of best focus. The bulk of the laser pulse (both radially over the focal spot and axially over several focal depths) therefore samples a uniform, fully ionized plasma of density $n_e = Zn_n$, where $Z = 2$ is the charge state and n_n is the neutral density of helium.

In Fig. 2 we show a typical backscatter spectrum obtained when the laser is operated at $I \cong 10^{18}$ W/cm^2. Such spectra were obtained for neutral helium pressures between 0.5 and 20.0 torr ($\pm 1\%$; $n_e = 3.3\times10^{16}$–1.3×10^{18} cm^{-3} if 100% ionization is assumed). In this figure the narrow spectral peak at 1.05 μm is the laser fiducial. The RBS spectrum exhibits two prominent features. The first is a broad redshifted peak which has a width greater than its shift and which extends to the blue side of the incident laser peak. This feature is only ob-

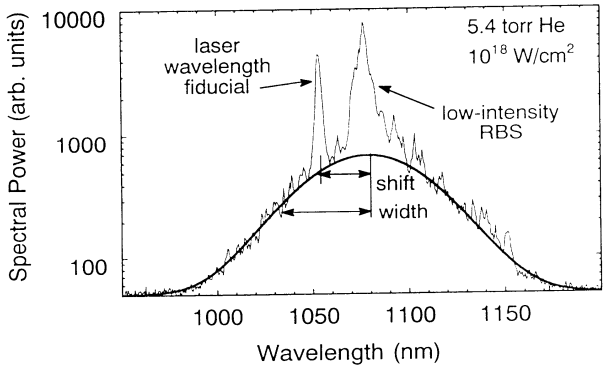

FIG. 2. Experimentally observed RBS spectrum at high laser intensity. The broad, nearly symmetric feature extending to the blue is observed only in high-intensity shots and is attributed to strongly coupled SRS. Heavy solid curve is Gaussian-plus-constant fit to the broad feature. The shift and width referred to in Fig. 3 are indicated.

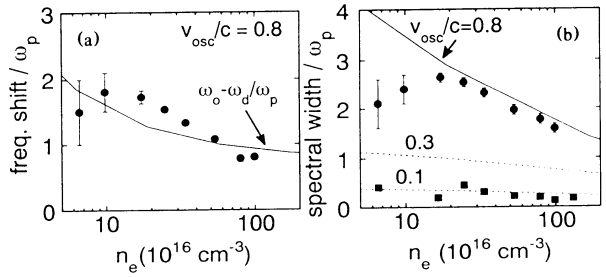

FIG. 3. (a) Theoretical ($\omega_0 - \omega_d$) and experimental frequency shifts of the broad red feature in the strongly coupled RBS spectra. (b) Spectral widths (solid line, theory; circles, high-power experiments; squares, low-power experiments) and maximum growth rates (dashed lines).

served for the highest-intensity shots (laser energy greater than 2 J). The second is an intense relatively narrow feature which has a shift somewhat greater than the plasma frequency of a fully ionized gas. Because it is common to spectra taken at both low and high intensities we attribute this narrow feature to weakly coupled RBS from regions of the focal volume where the intensity is low. Assuming the redshift of this peak is given by the Bohm-Gross frequency ω_{BG}, we infer a longitudinal electron temperature of 5 to 10 eV over the entire density range of the experiment.

The RBS signal falls below detection threshold when $n_e < 5\times10^{16}$ cm^{-3} for two reasons. First, Landau damping of the plasma waves becomes significant at the lower densities. For example, at $n_e = 10^{17}$ cm^{-3} the Landau damping rate is already $0.5\omega_p$. This causes the effective growth rate to be reduced. Second, the ponderomotive force of the laser is large enough to expel a significant number of electrons [11]. Equating the ponderomotive force to the space-charge force we find a density depression of

$$\frac{\delta n}{n} = \left(\frac{v_{osc}}{c}\right)^2 \frac{\lambda_0^2}{\sigma^2}\frac{\omega_0^2}{\omega_p^2}\frac{1}{4\pi^2}$$

(σ is the focal spot diameter and λ_0 is the laser wavelength) which approaches 50% at a density of 5×10^{16} cm^{-3} for $v_{osc}/c = 0.8$. On the other hand, for densities beyond 10^{19} cm^{-3} self-phase modulation of the light pulse caused by the ionization process can appreciably affect the incident light spectrum [12]. For this reason we present in this paper only data at densities up to 3×10^{18} cm^{-3} where such effects have been shown to contribute negligibly [13].

In Fig. 3(a) we compare the calculated ω_d for the mode with the largest growth rate with the shift of the broad feature observed in the measured high-intensity spectra. The experimental shifts are determined by fitting the broad feature with a Gaussian (plus a constant; heavy solid curve in Fig. 2). The experimental data are in qualitative agreement with the shifts predicted by the modified strong-coupling theory. In particular, the observed shifts are less than ω_p for the high densities. At the lowest density the measured frequency shifts are thought to be lower than the predicted values because electron blowout by the radial ponderomotive force of the laser reduces the electron density. On the other hand, inclusion of kinetic terms in the RBS dispersion relation will tend to increase the shifts for the lower densities because the modes with larger ω_r (and largest δ) are less severely Landau damped.

The broad bump seen in the high-intensity experiments is due to RBS driven by laser intensities for which the growth rate exceeds the Bohm-Gross frequency. This criterion is met only near best focus at the peak of the laser pulse. Therefore the number of e-foldings can be limited and the strongly coupled instability may not be driven to saturation. In this case we estimate the spectral widths from the width of the exponentiated ω_i vs ω_r curves [cf. Fig. 1(b)].

In Fig. 3(b) we plot the experimentally measured widths of the broad feature (circles) and the predicted widths for an e-folding time of $\omega_0 t = 100$ and $v_{osc}/c = 0.8$. This time corresponds to roughly three e-foldings for the fastest growing mode. The predicted widths agree quite well with the measured widths except at the lowest densities where it becomes difficult to obtain meaningful Gaussian fits (because the laser fiducial overlaps the red feature), though electron blowout could also reduce the measured widths. If instead $\omega_0 t = 500$ is assumed, the entire curve shifts down but remains considerably above the low-power widths. We emphasize that the widths predicted by a simple exponentiation of the ω_i vs ω_r curve would be too small by at least a factor of 2 and the resulting spectra would contain no blue component.

Another effect could also, in principle, broaden the spectrum of each individual ω and k mode. The Fourier spectrum of a growing exponential of the form $e^{i\omega t}e^{\Gamma t}$ is a

Lorentzian centered at frequency ω with a width of Γ. If the instability were not saturated, the spectrum of the detected signal could be broadened. In short-pulse experiments, however, the spatial pulse length is a small fraction of both the plasma size and the Rayleigh length. As a result, the signal grows because the intensity of the laser changes as the pulse passes through the focal volume. The resulting width Γ is estimated by differentiating $\exp(\int \gamma dt)$ with respect to z. This gives $\Gamma = -\frac{2}{3} zc\tau\gamma_0/(z^2+z_0^2)$, where γ_0 is the growth rate at best focus, z_0 is the Rayleigh length, and z is the axial position relative to best focus. For $c\tau < z_0$ the broadening is less than γ_0. In this experiment $c\tau$ is between $\frac{1}{2}$ and $\frac{1}{5}$ of z_0. Therefore, this transient broadening, on its own, fails to account for the large widths and blue component of the observed spectra, and does not in any case predict shifts smaller than ω_p at high densities.

As an aside we note that the width of the narrow feature in the low-power spectra (not shown here) provides a direct measure of the weak-coupling growth rates. The narrow peak is produced throughout the laser pulse by RBS which eventually saturates because the number of e-foldings is large. That saturation occurs can be seen by integrating the weakly coupled growth rate [14] $\gamma = (1/2\sqrt{2})(v_{\rm osc}/c)(\omega_0\omega_p)^{1/2}$ over the laser pulse. The number of e-foldings can be expressed as

$$N = \int dt\, \gamma = \frac{\pi}{2\sqrt{2}} \frac{v_{\rm osc}}{c} \left(\frac{\omega_p}{\omega_0}\right)^{1/2} \omega_0 t ,$$

where the temporal intensity profile is assumed to be Gaussian with a characteristic width t. For $v_{\rm osc}/c \cong 0.3$ (low intensity), $t = 800$ fs, and n_e between 10^{17} and 10^{18} cm^{-3}, $N = 50$–70, respectively. Clearly, for any reasonable thermal fluctuation level, the unstable modes will saturate before such a large number of e-foldings can occur. Assuming each mode has a similar saturated level, the spectral width should reflect the width of the ω_i vs ω_r curve which, as shown in Fig. 1(a), is equal to twice the temporal growth rate. We have therefore also plotted the maximum weak-coupling temporal growth rate for various laser intensities ($v_{\rm osc}/c$) as a function of density (the dashed lines) along with the measured widths of the low-power narrow feature in Fig. 3(b). The measured widths of the narrow feature are consistent with theoretical predictions for $v_{\rm osc}/c$ between 0.1 and 0.3, in good agreement with our best estimates of the laser intensity in the low-intensity experiments.

In conclusion, we have observed stimulated Raman backscattering from intense, subpicosecond laser-produced plasmas. At the highest intensities the backscattered spectra are consistent with strongly coupled Raman backscatter theory, appropriately modified for short pulses: The "red" features in the scattered spectra have widths greater than ω_p, extend to the blue side of the laser, and, at the highest densities, can be shifted by less than ω_p. At low intensity, the widths of the red feature, which provide a measure of conventional SRS growth rates, are consistent with theory.

This work was supported by DOE Contract No. DE-AS03-83-ER40120, DOE Grant No. DE-FG03-91ER12114 and LLNL University Research Program under tasks No. 11 and No. 25 at UCLA. We thank Dr. Wim Leemans, Dr. Tom Katsouleas, and Dr. William Kruer for many useful discussions.

[1] D. W. Forslund *et al.*, Phys. Fluids **18**, 1017 (1975); K. Estabrook and W. L. Kruer, Phys. Fluids **26**, 1982 (1983); W. L. Kruer *et al.*, Phys. Fluids **23**, 1326 (1980); W. B. Mori *et al.*, in *Laser Interaction and Related Plasma Phenomena*, edited by H. Hora and G. Miley (Plenum, New York, 1986), Vol. 7, pp. 241–258.

[2] D. W. Phillion *et al.*, Phys. Fluids **25**, 1434 (1982); K. Tanaka *et al.*, Phys. Rev. Lett. **48**, 1179 (1982); H. Figueroa *et al.*, Phys. Fluids **27**, 1887 (1984).

[3] P. Amendt *et al.*, Phys. Rev. Lett. **66**, 2589 (1991); D. C. Eder *et al.*, Phys. Rev. A **45**, 6761 (1992).

[4] P. Sprangle and E. Esarey, Phys. Rev. Lett. **67**, 2021 (1991).

[5] D. W. Forslund *et al.*, Phys. Fluids **18**, 1002 (1975); J. F. Drake *et al.*, Phys. Fluids **17**, 778 (1974).

[6] This is calculated by solving the RBS dispersion relation with the constraint $ck_i = \omega_i$.

[7] W. B. Mori, Phys. Rev. A **44**, 5118 (1991); R. L. Savage, Jr., *et al.*, Phys. Rev. Lett. **68**, 946 (1992).

[8] F. G. Patterson *et al.*, Opt. Lett. **16**, 1107 (1991).

[9] This intensity is consistent with observations of Ne^{8+} and Ar^{10+}; J. Crane (private communication). The v_0/c quoted is calculated nonrelativistically.

[10] W. P. Leemans *et al.*, Phys. Rev. Lett. **68**, 321 (1992); C. E. Clayton *et al.* (to be published).

[11] W. B. Mori *et al.*, Phys. Rev. Lett. **60**, 1298 (1988); G. Sun *et al.*, Phys. Fluids **30**, 526 (1987).

[12] W. M. Wood *et al.*, Phys. Rev. Lett. **67**, 3523 (1991).

[13] C. Darrow *et al.*, Bull. Am. Phys. Soc. **36**, 2303 (1991).

[14] This is the RBS growth rate in the $z-ct$ variable; see Ref. [4] and C. J. McKinstrie and R. Bingham, Phys. Fluids (to be published).